

HYPERONS IN NEUTRON STAR MATTER WITHIN RELATIVISTIC MEAN-FIELD MODELS

M. Oertel^{1,*}, *C. Providencia*², *F. Gulminelli*³, *A. R. Raduta*⁴

¹ LUTH, CNRS, Observatoire de Paris, Université Paris Diderot, Meudon, France

² Department of Physics, University of Coimbra, Coimbra, Portugal

³ ENSICAEN, UMR6534, LPC, Caen cédex, France

⁴ IFIN-HH, Bucharest-Magurele, Romania

Since the discovery of neutron stars with masses around $2M_{\odot}$, the composition of matter in the central part of these massive stars has been intensively discussed. Within this paper we will (re)investigate the question of appearance of hyperons. To that end, we will perform parameter study within relativistic mean-field models. We will show that it is possible to obtain high-mass neutron stars with a substantial amount of hyperons and a spinodal instability at the onset of hyperons. The results depend strongly on the interaction in the hyperon–hyperon channels, on which only very little information is available from terrestrial experiments up to now.

PACS: 97.60.Jd

INTRODUCTION

With the purpose of better understanding the dynamics of core-collapse supernova and the observed neutron star characteristics, a considerable theoretical effort has been undertaken in recent years concerning the modelization of the equation of state (EoS) of cold dense matter with some extensions to finite temperature.

If it is well admitted that hyperonic and deconfined quark matter could exist in the inner core of neutron stars, a complete understanding of its composition is far from being achieved. Concerning hyperons, simple energetic considerations suggest that they should be present at high density [1]. However, in the standard picture, the opening of hyperon degrees of freedom leads to a considerable softening of the EoS [1], which in turn leads to maximum neutron star masses smaller than the highest observed values [2]. This puzzling situation implies

*E-mail: micaela.oertel@obspm.fr

that the hyperon–hyperon (YY) and hyperon–nucleon (YN) couplings must be much more repulsive at high density than presently assumed (e.g., [3]) and/or that something is missing in the present modelization. The general agreement is that the price to pay for this additional repulsion is a very low strangeness content of neutron stars [3].

In addition, the generic presence of attractive and repulsive couplings suggests the existence, in a model-independent manner, of a phase transition involving strangeness. A detailed study of the phase diagram of dense baryonic matter was recently undertaken in [4, 5] within a nonrelativistic mean-field model based on phenomenological functionals. It was shown that under these assumptions first- and second-order phase transitions exist, and are expected to be explored under the strangeness equilibrium condition characteristic of stellar matter. In [6], such a phase transition has been discussed for relativistic mean-field models, but within a model with very strong YY attraction.

Here we are interested in (a) examining in which region of parameter space within RMF models a first-order phase transition from purely nuclear to hyperonic matter could exist, and whether the existence of such a phase transition is compatible with experimental and observational data, (b) whether it is possible to obtain high-mass neutron stars with considerable amount of hyperons.

1. THE MODEL

The literature on phenomenological RMF models including hyperons is large and many different versions exist (see, e.g., [7]), including either nonlinear couplings or density-dependent ones of baryons to the meson fields mediating the interaction. For the present study, we will limit ourselves to one nonlinear model, GM1 [8]. Its Lagrangian \mathcal{L} can be written as

$$\begin{aligned} & \sum_{j \in \mathcal{B}} \bar{\psi}_j (i\gamma_\mu \partial^\mu - m_j + g_{\sigma j} \sigma + g_{\sigma^* j} \sigma^* - g_{\omega j} \gamma_\mu \omega^\mu - g_{\phi j} \gamma_\mu \phi^\mu - g_{\rho j} \gamma_\mu \boldsymbol{\rho}^\mu \mathbf{I}_j) \psi_j + \\ & + \frac{1}{2} (\partial_\mu \sigma \partial^\mu \sigma - m_\sigma^2 \sigma^2) - \frac{1}{3} g_2 \sigma^3 - \frac{1}{4} g_3 \sigma^4 + \frac{1}{2} (\partial_\mu \sigma^* \partial^\mu \sigma^* - m_{\sigma^*}^2 \sigma^{*2}) - \\ & - \frac{1}{4} W_{\mu\nu}^\dagger W^{\mu\nu} - \frac{1}{4} P_{\mu\nu}^\dagger P^{\mu\nu} - \frac{1}{4} \mathbf{R}_{\mu\nu}^\dagger \mathbf{R}^{\mu\nu} + \frac{1}{2} m_\omega^2 \omega_\mu \omega^\mu + \frac{1}{2} m_\phi^2 \phi_\mu \phi^\mu + \frac{1}{2} m_\rho^2 \boldsymbol{\rho}_\mu \boldsymbol{\rho}^\mu, \end{aligned}$$

where ψ_j denotes the field of baryon j ; $W_{\mu\nu}, P_{\mu\nu}, \mathbf{R}_{\mu\nu}$ are the vector meson field tensors which are of the form $V^{\mu\nu} = \partial^\mu V^\nu - \partial^\nu V^\mu$, and σ, σ^* are scalar–isoscalar meson fields, coupling to all baryons (σ) and to strange baryons (σ^*), respectively.

In mean-field approximation, the meson fields are replaced by their respective mean-field expectation values, related to the baryonic scalar and number densities.

The effective baryon mass M_i^* depends on the scalar mean fields as $M_i^* = M_i - g_{\sigma i} \bar{\sigma} - g_{\sigma^* i} \bar{\sigma}^*$, and the effective chemical potentials, $(\mu_i^*)^2 = (M_i^*)^2 + k_{F_i}^2$, are related to the chemical potentials via $\mu_i^* = \mu_i - g_{\omega i} \bar{\omega} - (g_{\rho i}/2) t_{3i} \bar{\rho} - g_{\phi i} \bar{\phi}$. The resulting properties of homogeneous symmetric nuclear matter are $K = 300$ MeV, $E_{\text{sym}} = 32.5$ MeV, saturation density $n_0 = 0.153$ fm $^{-3}$, $B = -16.3$ MeV, and $L = 94$ MeV.

Setup for the Hyperonic Interaction. The wealth of nuclear data allows one to constrain the nuclear interaction parameters within reasonable ranges, whereas this is not the case for hyperons, where data are scarce. This leaves some freedom in adjusting the interaction parameters for the hyperonic sector.

Many recent works, see, e.g., [3], use a procedure inspired by the symmetries of the baryon octet to express the individual isoscalar vector meson–baryon couplings in terms of $g_{\omega N}$ and a few additional parameters. The α , thereby, determines the ratio of symmetric coupling of the baryons to the vector meson octet (D -term) and the antisymmetric coupling (F -term), $z = g_8/g_1$, the ratio of the coupling constants for baryons to the vector meson octet and singlet, respectively. The θ is the mixing angle of ω - and ϕ -mesons with the corresponding singlet and octet states. As is commonly assumed, in what follows, we will take $\tan \theta = 1/\sqrt{2}$, corresponding to ideal mixing and $\alpha = 1$. In the literature, mostly $SU(6)$ symmetry to fix the couplings, i.e., $z = 1/\sqrt{6}$, is imposed, and only recent studies in view of the observation of high-mass neutron stars have relaxed this assumption, for example [3]. In the isovector sector, not the same procedure is applied, since this would lead to contradictions with the observed nuclear symmetry energy. The $g_{\rho N}$ is therefore left as a free parameter, adjusted to the desired value of the symmetry energy, and the remaining isovector–vector couplings are obtained from $g_{\rho N}$ by isospin symmetry.

Within this framework, for the scalar sector, the information from hypernuclear data on hyperonic single-particle mean-field potentials is used to constrain the coupling constants. In particular, $g_{\sigma Y}$ are then adjusted to reproduce the hyperon potentials in symmetric nuclear matter. Based on hypernuclear data, the results presented below always assume $U_{\Lambda}^{(N)}(n_0) = -28$ MeV, $U_{\Xi}^{(N)}(n_0) = -18$ MeV, and $U_{\Sigma}^{(N)}(n_0) = 30$ MeV, see, e.g., [5] for a discussion.

Very few multihyperon exotic nuclei data exist so far and all of them correspond to double- Λ light nuclei, suggesting $U_{\Lambda}^{(\Lambda)}(n_0/5) \approx -5$ MeV as most attractive value. The Nagara event [10] is even in favor of a much less attractive one, $U_{\Lambda}^{(\Lambda)}(n_0/5) \approx -0.7$ MeV. For the other potentials it is often assumed that in isospin symmetric Ξ - and Σ -matter, $U_{\Xi}^{(\Xi)}(n_0) \approx 2U_{\Lambda}^{(\Lambda)}(n_0/2)$ and $U_{\Sigma}^{(\Sigma)}(n_0) \approx U_{\Lambda}^{(\Lambda)}(n_0/2)$ [9] based on theoretical estimates. In view of the only weakly attractive $\Lambda\Lambda$ -potential and the uncertainties on other hyperon–hyperon (YY) potentials, often σ^* is neglected (see, e.g., [3]).

2. RESULTS AND DISCUSSION

We are interested here in sets of couplings describing stellar matter with an instability at the onset of hyperons. The existence of a first-order phase transition can be spotted by analyzing the curvature of a thermodynamic potential in terms of extensive variables, indicating the presence of a spinodal instability related to the phase transition. The unstable region is thereby recognized by a negative curvature. We will follow here the procedure described in detail in [5], analyzing the eigenvalues of the curvature matrix, $C_{ij} = \partial^2 \varepsilon(\{n_l\}_{l=\{i,j,k\}}) / \partial n_i \partial n_j$, where $i, j, k = B, S, L$. In all our studies at most one negative eigenvalue has been found.

Following the above-described procedure, once z is fixed, the only remaining parameters are the couplings to σ^* . In Fig. 1, *a*, we show the minimal eigenvalue of the curvature matrix, c_{\min} , as a function of baryon number density in neutron star matter for different choices of the couplings to σ^* and z . In the curves, the successive thresholds, leading to kinks in c_{\min} , can be observed. They correspond to the onset Λ^- , Ξ^- , and Ξ^0 -hyperons, respectively. The Σ -hyperons appear only well above $n_B = 1 \text{ fm}^{-3}$, beyond the central density of the neutron stars with the highest mass.

In the Table, we list the values of $U_Y^{(Y)}(n_0/5)$ corresponding to the different parameter choices. It is evident that the system is perfectly stable for those giving the canonical values $U_\Lambda^{(\Lambda)}(n_0/5) = -5 \text{ MeV}$ and $U_\Xi^{(\Xi)}(n_0/5) = -10 \text{ MeV}$. Increasing g_{σ^*i} , however, decreases the minimal eigenvalue of the curvature matrix leading finally to an instability. Results are displayed, too, with the smallest value of $g_{\sigma^*\Lambda}$ and $g_{\sigma^*\Xi}$, respectively, leading to an instability. As can be seen, an instability shows up for lower values of $g_{\sigma^*\Xi}$ for Ξ^0 than for Ξ^- .

The YY -interaction is very sensitive to the couplings to σ^* . Remember that originally the σ^* has been introduced [9] to allow for very attractive YY -interactions. A large value of g_{σ^*Y} indeed induces a strong attraction, as seen from the values for $U_\Xi^{(\Xi)}(n_0/5)$ and $U_\Lambda^{(\Lambda)}(n_0/5)$ listed in the Table. It is obvious, that the attraction needed in the $\Lambda\Lambda$ -channel to obtain an instability is much higher for all examples shown than the values suggested by experimental data. In the $\Xi\Xi$ -channel and the $\Sigma\Sigma$ -channel, the situation is less evident because there is no experimental information available in these channels. Current information, based on theoretical arguments for the baryon octet in vacuum and corresponding meson exchange models, is clearly not sufficient to pin down the amount of attraction for the YY -interaction in dense matter. Since the coupling to σ^* is determined mainly via the YY -interaction, more data, and on other hyperons than Λ -hyperons, would be very welcome to be able to judge whether the different chosen values are pertinent or not.

In the Table, the maximum mass, the radius at a gravitational mass of $1.4M_\odot$, and the radius at maximum mass for spherical nonrotating neutron stars are

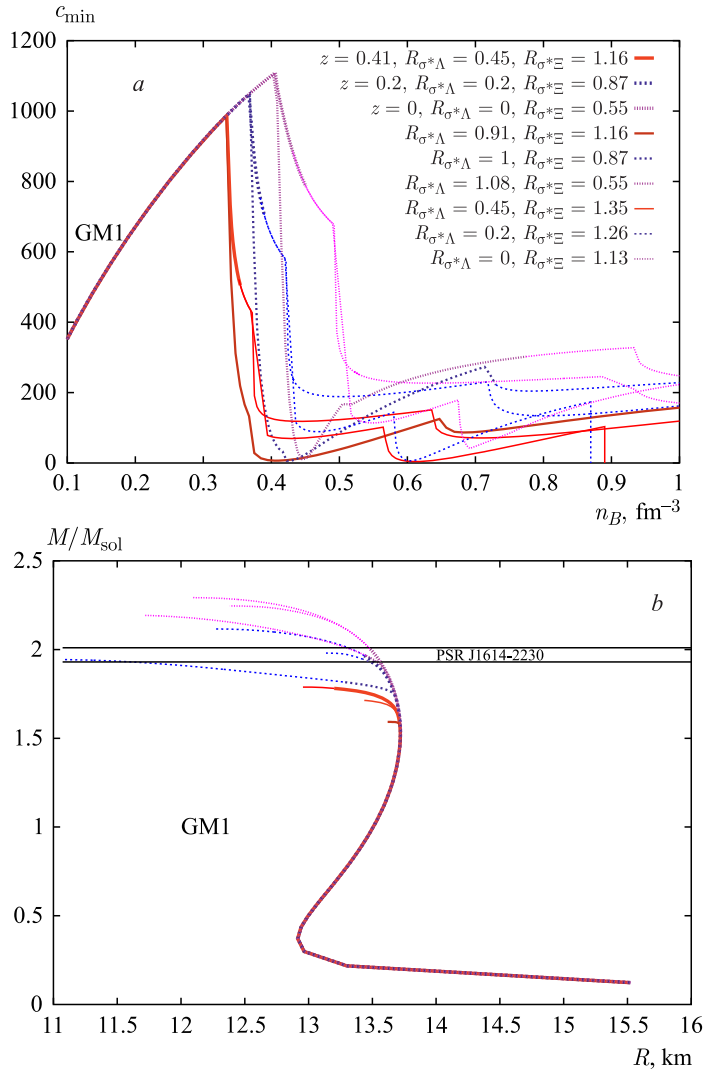


Fig. 1. *a*) The smallest eigenvalue of the curvature matrix of the energy density as a function of baryon number density for neutron star matter for different parameter sets. *b*) (Gravitational) mass/radius curves for spherical neutron stars for the above choice of parameters. The interaction parameters are indicated in the legend of the figures

given for the different parameter sets discussed in the preceding section. In Fig. 1, *b*, the corresponding mass-radius relations are plotted. We observe that upon decreasing z , the maximum mass increases, and that upon increasing both

Summary of results. The central strangeness fraction $Y_s = n_S/n_B$ is given for the maximum mass configuration

z	$M_{\max},$ M_{\odot}	$R_{1.4},$ km	$R_{\max},$ km	$Y_S^{(c)}$	f_S	$R_{\sigma^*\Lambda}$	$R_{\sigma^*\Xi}$	$U_{\Lambda}^{\Lambda}(n_0/5),$ MeV	$U_{\Xi}^{\Xi}(n_0/5),$ MeV
0.41	1.79	13.7	13.0	0.70	0.04	0.45	1.16	-5	-10
0.41	1.59	13.7	13.6	0.59	0.006	0.91	1.16	-44	-10
0.41	1.71	13.7	13.4	0.75	0.02	0.45	1.35	-5	-21
0.2	2.12	13.7	12.3	0.71	0.07	0.20	0.87	-5	-10
0.2	1.94	13.7	11.0	0.93	0.20	1.0	0.87	-27	-10
0.2	1.98	13.7	13.1	0.84	0.03	0.20	1.26	-5	-29
0.	2.29	13.7	12.1	0.46	0.04	0	0.55	-7	-10
0.	2.19	13.7	11.7	0.64	0.12	1.08	0.55	-34	-10
0.	2.24	13.7	12.4	0.76	0.05	0	1.13	-7	-33

σ^* -couplings, to Λ - and Ξ -hyperons, leading to a stronger attraction, the maximum mass decreases. This is perfectly understandable, since a smaller z means a stronger repulsion and a larger coupling to σ^* induces stronger attraction. The effect of increasing the attraction due to a σ^* -coupling between the canonical and the critical value is more pronounced for the threshold to Λ -hyperons than for the Cascades. The reason is that the difference between the canonical and the critical value in the Cascade channel is smaller than for the Λ -hyperons, partly because at the Cascade thresholds other hyperons are already present pushing the instability.

From all the above-discussed examples, it is clear that the existence of an instability is not excluded by the neutron star maximum masses. The maximum masses are more strongly dependent on the vector couplings than on the σ^* -couplings for values between zero and the critical values, such that the allowed parameter space is still large.

In Fig. 2, we display the fractions of the different particles in neutron star matter as a function of baryon number density. As expected, rendering the vector repulsion stronger by decreasing z , the hyperon thresholds are shifted to higher densities. Thereby, the Cascade thresholds show a stronger z -dependence than the Λ -threshold. The reason is the stronger z -dependence of the individual hyperon-meson coupling constants, induced by the symmetry requirements of the procedure applied. It can be observed that all threshold densities for $z < 0.41$ are significantly lower than those in [3], i.e., hyperons are present at much lower baryon number densities. This can be explained by a different readjustment of the couplings to σ : we keep the values of the hyperon potentials in nuclear matter constant upon changing the value of z . In addition, all the curves have been calculated with nonzero coupling to σ^* .

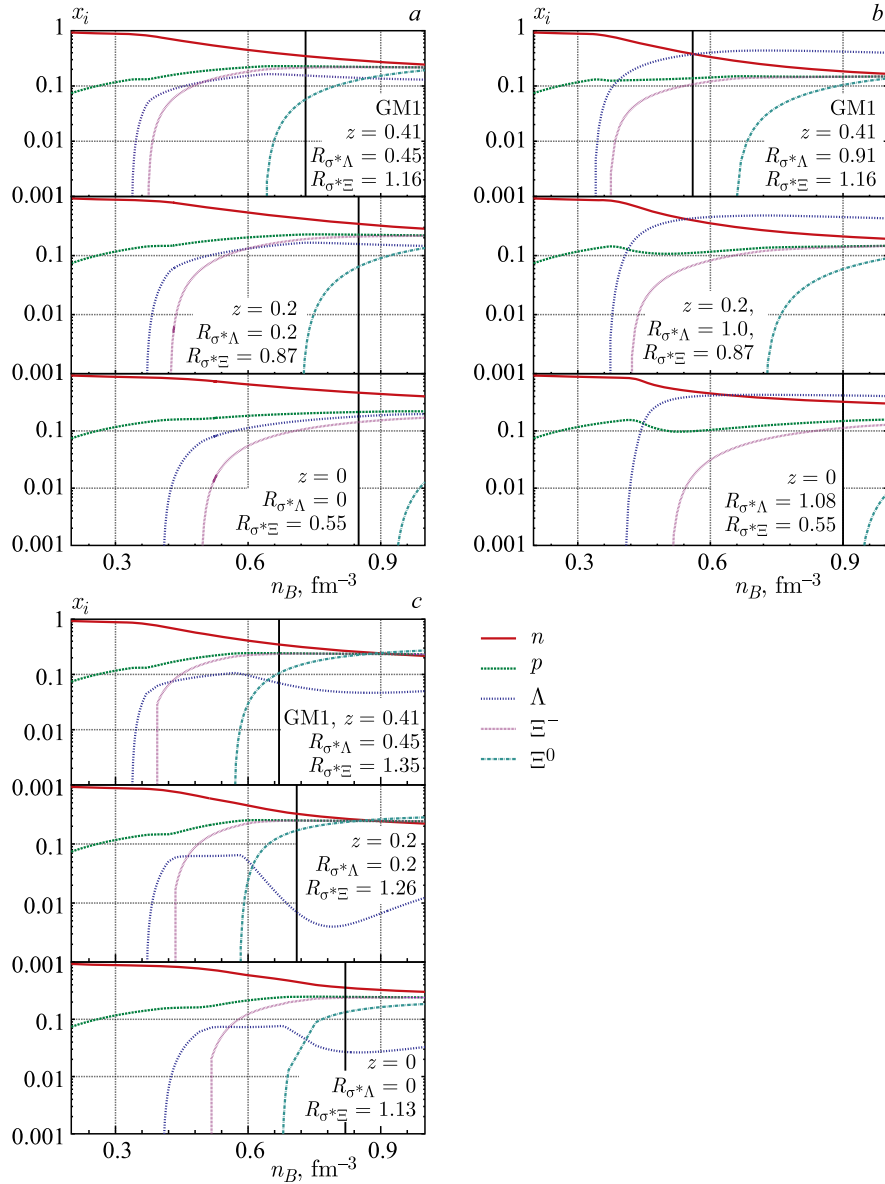


Fig. 2. Particle fractions in neutron star matter for the different parameter sets discussed above. The vertical lines indicate the central density of the respective maximum mass configurations

The observed dependence on the attraction furnished by σ^* is no surprise. Increasing g_{σ^*i} , the threshold density for hyperon i is lowered and its abundance is globally increased. In particular, on the panel c it can be seen that for a large $g_{\sigma^*\Xi}$, although, due to the much higher mass of the Cascades with respect to Λ , the latter threshold still remains the lowest one, at densities beyond the Ξ^0 -threshold, Λ -hyperons become the less abundant ones. This is again an example which shows to which extent the composition of the NS core depends on the interactions between different particles. Therefore, since the coupling to σ^* is determined mainly via the YY -interaction, more data, and on other hyperons than Λ -hyperons, would be very welcome to pin down the neutron star composition.

3. SUMMARY AND CONCLUSIONS

The possibility of instabilities driven by the onset of hyperons in the interior of neutron stars was investigated within an RMF approach. For the nucleonic part, we have considered the GM1 parameterization [8]. Concerning the hyperonic couplings, for the isoscalar vector ones, symmetry constraints have been imposed, relaxing, however, the $SU(6)$ -constraint. The YN scalar couplings have been adjusted to the existing experimental data. The g_{σ^*i} , strongly influencing the YY -interaction, have been varied freely, and, in particular, they have been chosen strong enough to originate an instability with the onset of hyperons.

It was shown that a correct choice of the coupling parameters, g_{σ^*i} , allowed for EoS giving neutron star masses as high as $2M_\odot$, with the particularity that instabilities occur at the onset of hyperons. In particular, it was shown that it is possible to have an instability driven by the onset of the Λ , or the Ξ depending on the choice of the coupling parameters. Presently, the scarce amount of experimental information on the hyperon sector, leaves too much freedom in adjusting the interaction parameters, which will only be restricted with more experimental data.

REFERENCES

1. *Glendenning N.* The Hyperon Composition of Neutron Stars // *Phys. Lett. B.* 1982. V. 114. P. 392.
2. *Demorest P. et al.* Shapiro Delay Measurement of a Two-Solar-Mass Neutron Star // *Nature.* 2010. V. 467. P.1081;
Antoniadis J. et al. A Massive Pulsar in a Compact Relativistic Binary // *Science.* 2013. V. 340. P. 6131.
3. *Weissenborn S., Chatterjee D., Schaffner-Bielich J.* Hyperons and Massive Neutron Stars: Vector Repulsion and $SU(3)$ Symmetry // *Phys. Rev. C.* 2012. V. 85. P. 065802.
4. *Gulminelli F., Raduta Ad. R., Oertel M.* Phase Transition Towards Strange Matter // *Phys. Rev. C.* 2012. V. 86. P. 025805;
Gulminelli F. et al. Strangeness-Driven Phase Transition in (Proto-)Neutron Star Matter // *Phys. Rev. C.* 2013. V. 87. P. 055809.

5. *Raduta A.R., Gulminelli F., Oertel M.* Thermodynamics of Baryonic Matter with Strangeness within Nonrelativistic Energy Density Functional Models. [arxiv.org:1406.0395](https://arxiv.org/abs/1406.0395).
6. *Schaffner-Bielich J., Gal A.* Properties of Strange Hadronic Matter in Bulk and in Finite Systems // *Phys. Rev. C.* 2000. V. 62. P. 034311.
7. *Dutra M. et al.* Relativistic Mean-Field Hadronic Models under Nuclear Matter Constraints // *Phys. Rev. C.* 2014. V. 90. P. 055203.
8. *Glendenning N.K., Moszkowski S.A.* Reconciliation of Neutron Star Masses and Binding of the Λ in Hypernuclei // *Phys. Rev. Lett.* 1991. V. 67. P. 2414.
9. *Schaffner J. et al.* Multiply Strange Nuclear Systems // *Ann. Phys.* 1994. V. 235. P. 35.
10. *Nakazawa K. et al.* Double- Λ Hypernuclei via the Ξ -Hyperon Capture at Rest Reaction in a Hybrid Emulsion // *Nucl. Phys. A.* 2010. V. 835. P. 207.